Results of the HySafe CFD Validation Benchmark SBEPV5

T. Jordan[1], J.García[3], O. Hansen[4], A. Huser[7], S. Ledin[8], P. Middha[4], V. Molkov[5], J. Travis[2], A.G. Venetsanos[6], F. Verbecke[5],J. Xiao[1]

[1]Forschungszentrum Karlsruhe GmbH Germany, [2]Ingenieurbüro DPT Germany, [3]Universidad Politecnica de Madrid Spain,[4]GexCon AS Norway, [5]University of Ulster United Kingdom, [6]National Center for Scientific Research Demokritos Greece, [7]Det Norsk Veritas Norway, [8]HSE/HSL United Kingdom

Corresponding author: Thomas.Jordan@iket.fzk.de

Session: Hydrogen Risk Assessment and Management

Keywords: hydrogen release, mixing and distribution

Abstract

The different CFD tools used by the NoE HySafe partners are applied to a series of integral complex Standard Benchmark Exercise Problems (SBEPs). All benchmarks cover complementarily physical phenomena, addressing application relevant scenarios, and refer to associated experiments with an explicit usage of hydrogen. After the blind benchmark SBEPV1 and SBEPV3 with subsonic vertical release in a large vessel and in a garage like facility, SBEPV4 with a horizontal under-expanded jet release through a small nozzle, SBEPV5 covers the scenario of a subsonic horizontal jet release in a multi-compartment room.

As the associated dispersion experiments conducted by GEXCON, Norsk Hydro and STATOIL were disclosed to the participants the whole benchmark was conducted openly. For the purpose of validation, only the low momentum test D27 had to be simulated.

The experimental rig consists of a 1.20 m x 0.20 m x 0.90 m (Z, vertical) vessel, divided into 12 compartments, partially even physically by four baffle plates. In each compartment a hydrogen concentration sensor is mounted. There is one vent opening at the wall opposite the release location centrally located about 1 cm above floor with dimensions 0.10 m (Y) times 0.20 m (Z). The first upper baffle plate close to the release point is on a sensitive location as it lies nearly perfectly in the centre of the buoyant jet and thus separates the flow into the two compartments. The actual release was a nominally constant flow of 1.15 norm liters for 60 seconds. With a 12mm nozzle diameter this corresponds to an average exit velocity of 10.17 m/s.

6 CFD packages have been applied by 7 HySafe partners to simulate this experiment: ADREA-HF by NCSRD, FLACS by GexCon and DNV, KFX by DNV, FLUENT by UPM and UU, CFX by HSE/HSL, and GASFLOW by FZK. The results of the different participants are compared against the experimental data. Sensitivity studies were conducted by FZK using GASFLOW and by DNV applying KFX.

Conclusions based on the comparisons and the sensitivity studies related to the performance of the applied turbulence models and discretisation schemes in the release and diffusion phase are proposed. These are compared to the findings of the previous benchmark exercises.

1. MOTIVATION

Hydrogen jets in closed spaces are typical ingredients of scenarios encountered in risk analyses for the future use of hydrogen as an anergy carrier. For comparing numerical models and their implementation the Network of Excellence (NoE) HySafe [1] dedicated several benchmark excersises to this category of mixing phenomena. However, so far mainly vertical jets of hydrogen in air were considered (SBEPV1, SBEPV3). The SBEPV4 benchmark relied on an experiment with a small supersonic, underexpanded horizontal jet. However this jet was free and the focus of this exercise was more on the modelling of the expansion area of the jet. This paper documents the fifth standard benchmark example problem (SBEPV5), which addresses the dispersion phenomena implied with a low momentum horizontal hydrogen jet release in a multi-compartment room. After describing the experiment itself, the computational results will be compared and some conclusion will be presented.

2. THE EXPERIMENTAL SET-UP OF GEXCON D27

In 2003 GexCon, Norsk Hydro (both HySafe partners) and STATOIL have performed hydrogen dispersion experiments in a confined compartmented space. From a larger series the tests D06, D27 and D58 are shared within the HySafe network. For the purpose of code validation, the test D27 has been selected as a standard benchmark exercise problem.

The test D27 is characterised by a comparatively small geometrical scale.The experimental rig consists of a 1.20 m × 0.20 m × 0.90 m vessel (width X × depth Y × height Z), divided into compartments by use of baffle plates with dimensions 0.30 m (Z) × 0.20 m (Y). Four vertical baffle plates were used in test D27 (see Figure 1). There is one vent opening at the wall opposite the release location centrally located about 1 cm above floor with dimensions 0.10 m (Y) × 0.20 m (Z). The confinement could be characterised as a partial to full confinement, the congestion provided by the baffle plates is moderately high.

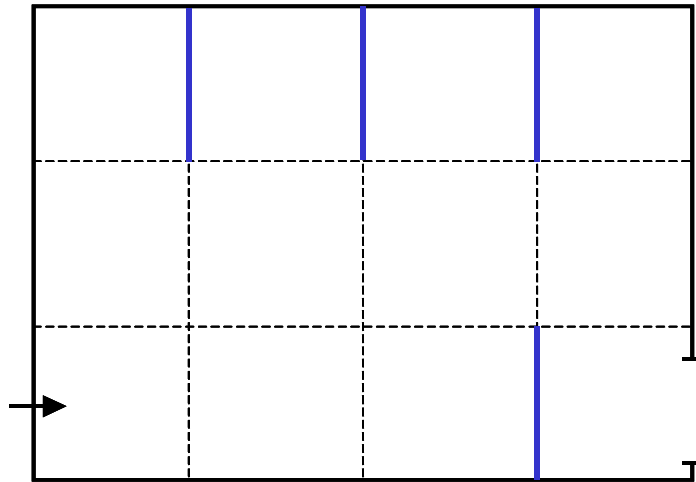**Figure 1. Photo of the GexCon test rig for test D27**

Figure 2. Geometry configuration of test D27

The release conditions and exact location of the jet exit for the selected test are given in Table 1 below.

Test ID	Release period (s)	Nozzle diameter (mm)	Exit velocity (m s^{-1})	Flow rate (Nl s^{-1})	X_{jet} (m)	Y_{jet} (m)	Z_{jet} (m)
D27	60	12	10.17	1.15	0.03	0.1	0.145

Table 1: Release conditions

The gas supply was fed to the experiment by means of a high pressure hose (1/4") via an electrically controlled solenoid "release" valve, located just upstream of the release nozzle. Prior to a dispersion test, this gas line was pressurised to the desired dispersion line pressure and the actual gas release controlled automatically by the test sequence control and data acquisition system, which opened and closed this "release" valve according to the desired release duration. There was no bend but a restriction through the valve. Also, for the test D27, the gas tested was pure H_2.

Hydrogen concentrations were recorded at 12 locations in the rear wall (see Figure 4), using Oldham sensors type OLCT20D [2]. The sensors are of the chatarometric type, which means that they are based on the measurement of the thermal conductivity of hydrogen compared to air. According to their specification they provide an accuracy of 1 vol % H_2 over the full range of 0-100 vol %.
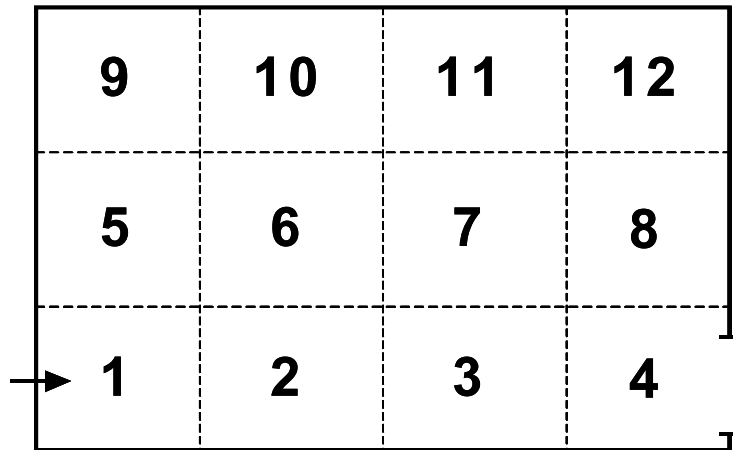
Figure 4. Sensor positions

Through the test series some problems with the gas concentration measurements were experienced for certain sensors (3, 6, 11). A negative concentration was often seen for a short period before sensors "recovered" and seemed to give good results. Sensor 4 frequently became unstable, and is suspected to give consistently poor results. Some tests were carried out swapping sensors, and these confirmed poor behaviour of the mentioned sensors.

3. THE EXPERIMENTAL RESULTS OF D27

The benchmark SBEPV5 was an open benchmark meaning that all participants had access to the experimental results from start on. The available dataset consists of transient volumetric hydrogen concentration recordings in MS EXCEL format for the 12 monitor locations for the first 120 s.

The following plots show the volumetric hydrogen (gas) concentrations versus time for the 8 reliable of the 12 monitor points. The measurements at the monitoring points 3, 4, 6, and 11 are ommitted due to the described problems. Figure 5.a shows the values obtained for sensors at the locations 1 and 2, Figure 5.b at location 5, 7, and 8, and Figure 5.c at location 9, 10, and 12. For these sensors, it is important to realise that the concentration for sensor 12 begins to increase much later compared to sensors 9 and 10. The explanation is simply that the domain where sensor 12 is located has the largest distance from the release point and that the domains 9 and 10 have to be filled first before hydrogen might flow into this area.
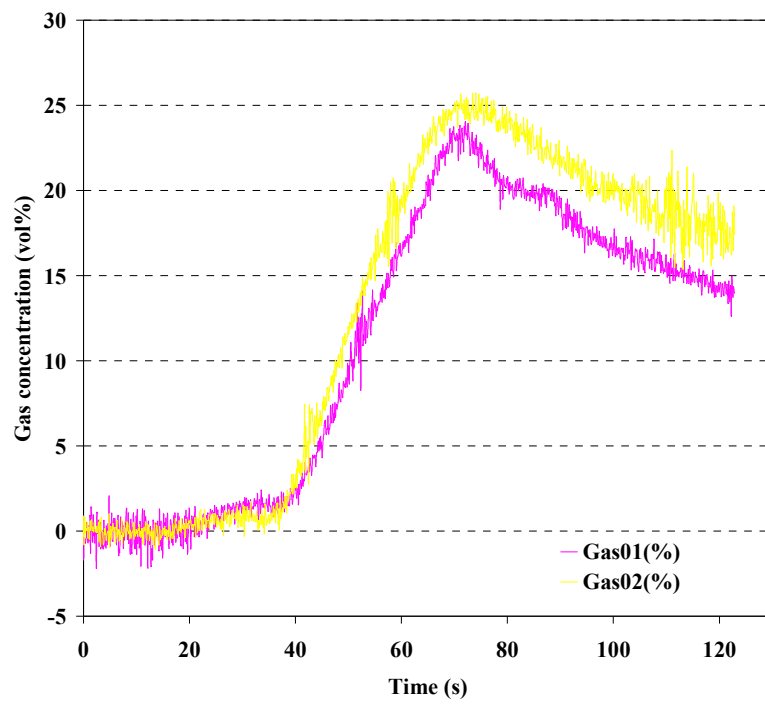
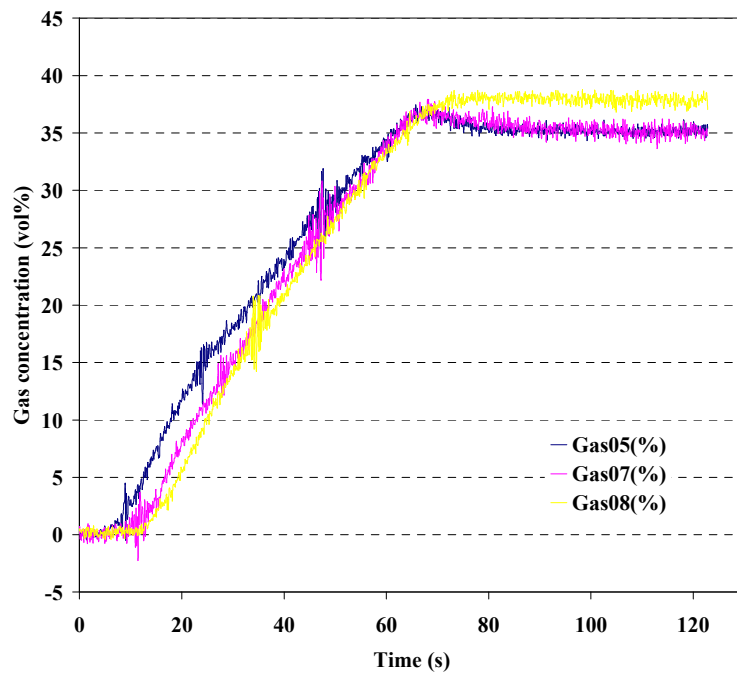**Figure 5.a Hydrogen concentration versus time for sensors 1 and 2**

Figure 5.b Hydrogen concentration versus time for sensors 5, 7, and 8
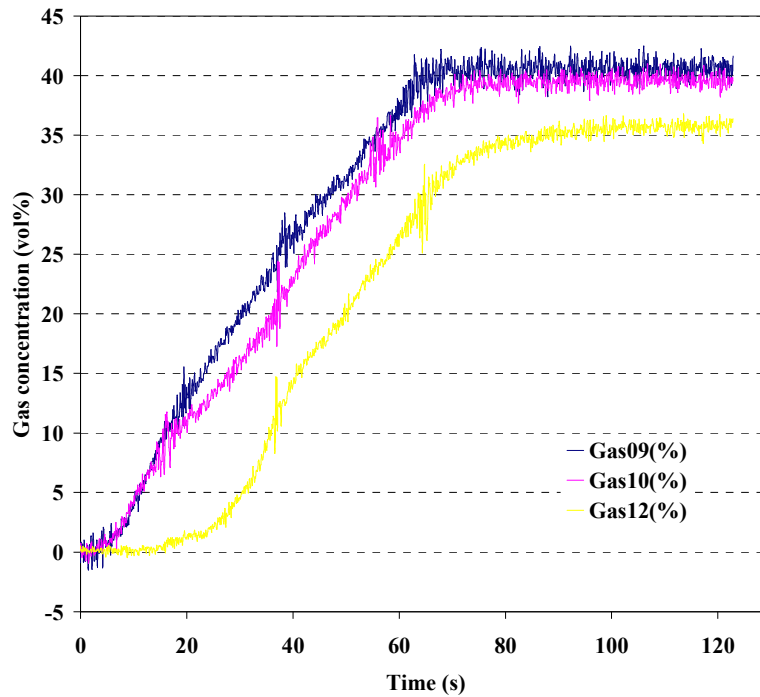
Figure 5.c Hydrogen concentration versus time for sensors 9, 10, and 12

4. SIMULATIONS

The following 3D CFD packages have been applied by 7 HySafe partner to simulate this experiment:

- ADREA-HF by NCSRD,
- FLACS by GexCon and DNV,
- KFX by DNV,
- FLUENT by UPM and UU,
- CFX by HSE/HSL, and
- GASFLOW by FZK.

In the following some details of the partners' simulations including the small sensitivity analyses of DNV and FZK are described.

4.1. *Numerical modeling of NCSRD*

Symmetry was not assumed. The grid (see Figure 6) was Cartesian equidistant with cell size equal to 0.012 m over most of the domain. Only outside the vessel the X grid expanded with a ratio of 1.12. The total number of cells was 113x17x76 in the X, Y, Z directions respectively. The total number of active cells was 141466. The source was modelled as an area source directed horizontally with the conditions shown in Table 1.

Calculations have been performed with the ADREA-HF code [3], using the standard k-ε model [4] extended for buoyant flows. A value of 0.7 was used for turbulent Schmidt number.

The first order upwind scheme was used for discretization of the convective terms. The first order Euler fully implicit scheme [5] was used for time discretization, with a maximum Courant number of 10.
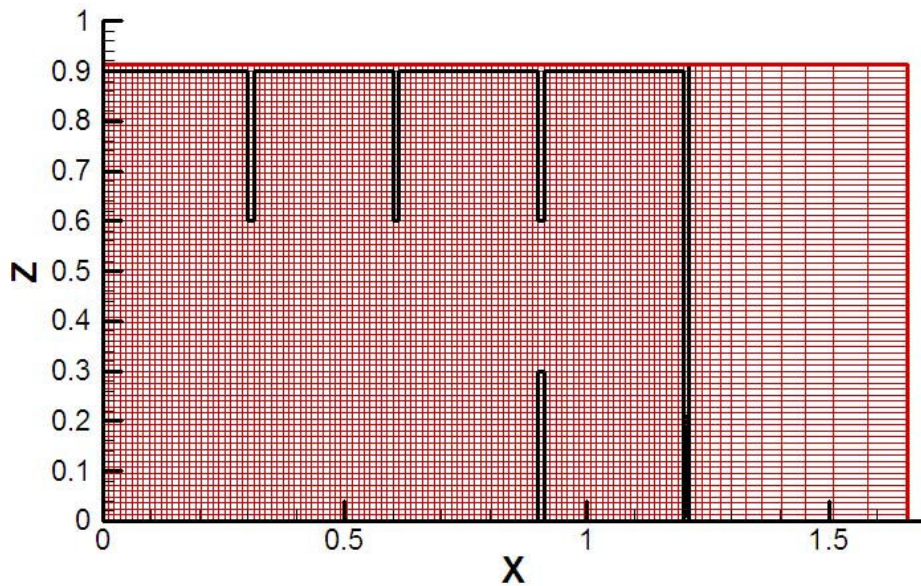

Figure 6 Grid on X-Z plane for ADREA-HF (NCSRD)

4.2.   *Numerical Modeling of GexCon*

The commercial version of FLACS, FLACS v8.1, released in March 2005, was applied for the study. The results have been generated with the FLACS postprocessor FLOWVIS.

There exist guidelines that must be followed for the time stepping in FLACS in order to get accurate results. These are using CFL-numbers based on speed of sound (CFLC) and flow velocity (CFLV). For explosion calculations CFLC=5 and CFLV=0.5 must be applied (which means that the pressure can propagate 5 cells and the flow 0.5 cells in each time step) to achieve good results. For dispersion calculations, the guidelines are less strict as results do not depend too much on the time steps. Normally it is recommended to increase the time steps by a factor of 4 (CFLC=20 and CFLV=2). When grid is refined near leak, it is also recommended to ignore the refined region (i.e. multiply CFLC-number with the refinement factor). But in practice, the CFL numbers can be even higher, leading to longer time steps, to get a reasonable simulation time. These long time steps and large grid aspect ratios will sometimes lead to instabilities, and therefore, the results need to be studied critically, and if instabilities are suspected (or simulation stops due to mass residual) it should be restarted with shorter time steps (divide CFLC and CFLV by two).
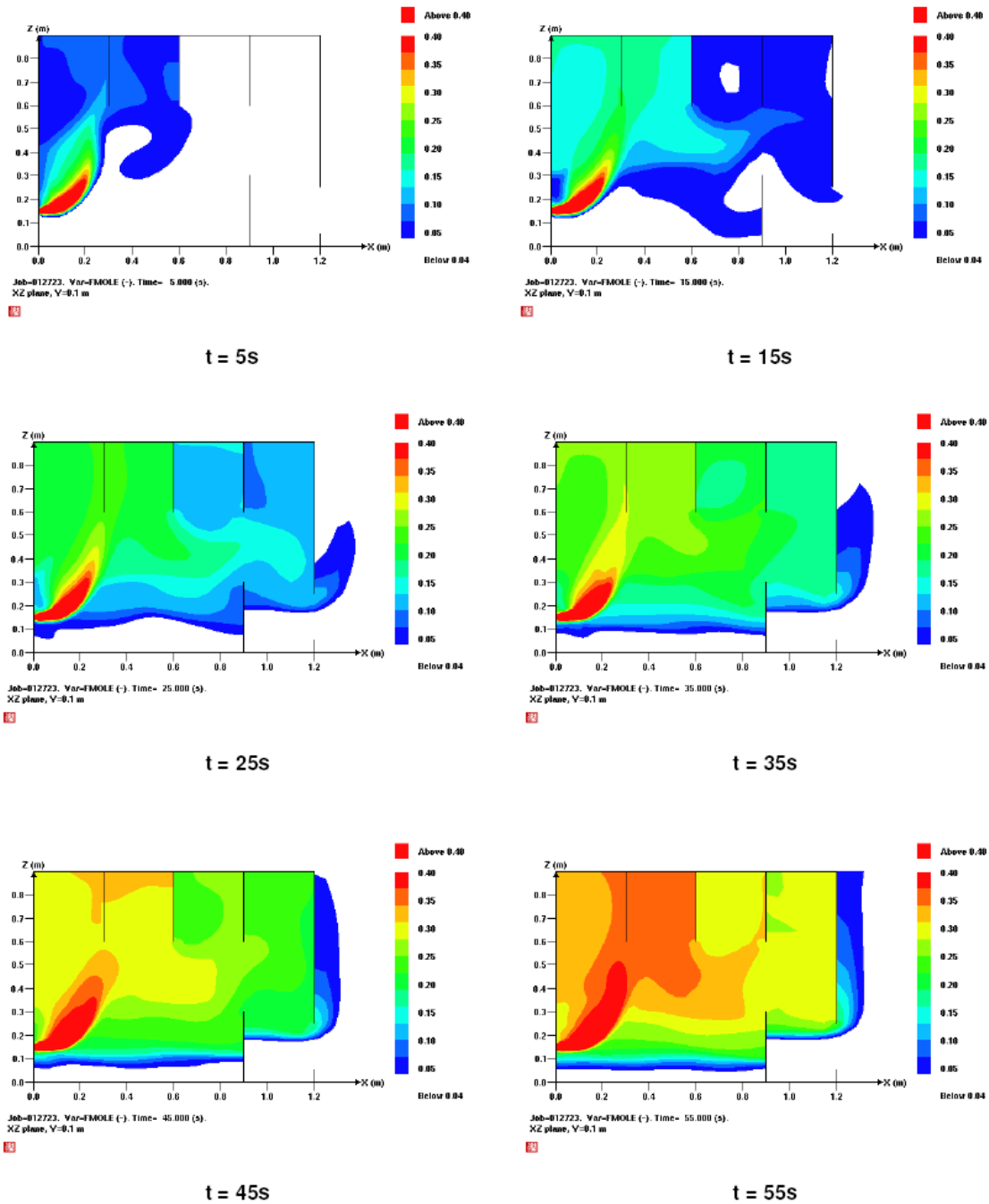
Figure 7 Concentration field in the middle XZ section at several time steps during the 60s release phase calculated with FLACS (GexCon)

Normally, it is recommended to refine the grid only around the jet, and not along it. This implies that if the leak direction is +X, the grid only needs to be refined in Y and Z direction. But in this case, the grid was also refined in X direction, owing to the high buoyancy of hydrogen. The grid should be refined in a 3-5 CV region around the leak, and then gradually smoothed. Poor results are seen without this refinement. The grid consisted of 38318 cells. The computation on a Linux PC with 2-3 GHz CPU with 2GB RAM needed 64 h CPU time.

4.3. *DNV Numerical simulations*

The experiment is simulated with two CFD codes: FLACS and KFX. The grid, boundary conditions and jet conditions are the same for both CFD programs in order to compare the results from the programs against each other.

The outflow of the jet is modelled with a temperature and pressure of 20 C and 1.01325 bar, respectively. The release velocity is 10.17 m/s, which gives a mass flow of $9.64 \times 10\text{-}5$ kg/s H_2 corresponding to the values in Table 1. The release is maintained the first 60 seconds of the simulation, then the release was stopped and the simulation continued until 120 seconds. The Reynold's number is 1130 corresponding to laminar flow.

The Courant number used in the simulations is around 0.7. It was found that the default Courant number at 10 in KFX was too coarse for this low-velocity jet. It was also found that lower Courant number than 0.7 gave similar results. For high velocity jets, the default Courant number of 10 in KFX is sufficient. In FLACS it was found that the CFLC number of 20 gave very strict time stepping for this case, leading to a very long computational time. The CFLC number was 300 in the simulations. Hence, the time steps are predicted only by the CFLV number, which was 0.7 corresponding to KFX. This is accurate for this low velocity jet. For high velocity jets, a CFLC and CFLV number of 20 and 2 should be used.

The vent opening is modelled as a pressure boundary condition, and the walls have a no slip condition with zero roughness.

A grid sensitivity study is performed in KFX order to find a grid independent solution. Three different grids were tested; a coarse grid with 0.1 m maximum cell length, a medium grid with 0.033 maximum cell length and a fine grid with a 0.011 m maximum cell length. All of the grids have the same size of the leak area. The leak cell is 0.011 m (Y) × 0.011 m (Z) for all grids, but the length of the leak cell (in X-direction) was 0.03 m for coarse and medium grid and 0.01 m for fine grid. The grids are stretched from the leak cell to the maximum cell length with a maximum stretch factor of 20%. The coarse, medium and fine grid have 4875, 15444 and 167751 cells, respectively.

The concentration of hydrogen at monitor point 6 is shown in Figure 8. Only small variations are seen, so it is not necessary to use the finest grid for this case. This is due to low velocity laminar flow, low gradients and simple geometry. The medium grid is further used for both FLACS and KFX.
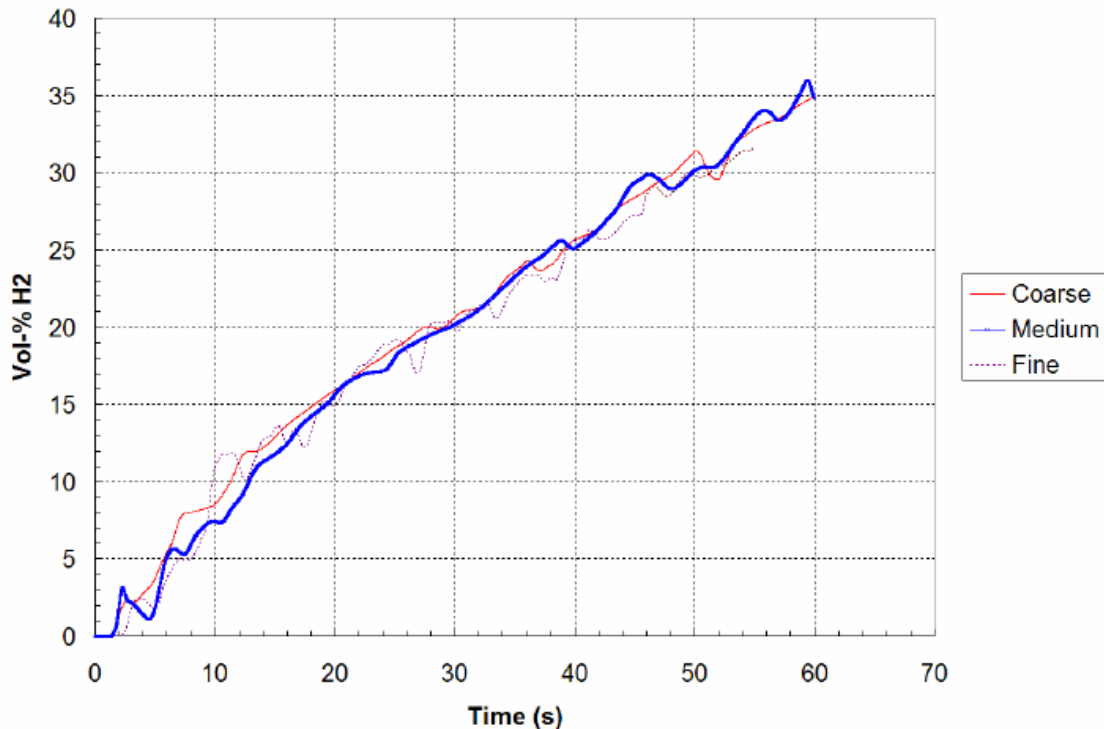

Figure 8 Concentration of H2 at monitor point 6 for three different grids used in KFX

4.4.   Numerical Modeling of UPM

The UPM has used the Fluent 6.2 code to simulate the SBEPV5 experiment. The standard k-ε turbulence model during the release and a laminar diffusion model after the release have been used. The governing equations for the turbulence model are the following:

$$\frac{\partial \rho}{\partial t} + \nabla \cdot (\rho \vec{v}) = S_m$$

$$\frac{\partial}{\partial t}(\rho \vec{v}) + \nabla \cdot (\rho \vec{v}\vec{v}) = -\nabla p + \nabla \cdot (\overline{\overline{\tau}}) + \rho \vec{g} + \vec{F}$$

$$\frac{\partial}{\partial t}(\rho k) + \frac{\partial}{\partial x_i}(\rho k u_i) = \frac{\partial}{\partial x_j}\left[\left(\mu + \frac{\mu_t}{\sigma_k}\right)\frac{\partial k}{\partial x_j}\right] + G_k + G_b - \rho \epsilon - Y_M + S_k$$

$$\frac{\partial}{\partial t}(\rho \epsilon) + \frac{\partial}{\partial x_i}(\rho \epsilon u_i) = \frac{\partial}{\partial x_j}\left[\left(\mu + \frac{\mu_t}{\sigma_\epsilon}\right)\frac{\partial \epsilon}{\partial x_j}\right] + C_{1\epsilon}\frac{\epsilon}{k}(G_k + C_{3\epsilon}G_b) - C_{2\epsilon}\rho\frac{\epsilon^2}{k} + S_\epsilon$$

The classical values for the constants have been used:

$$C_{1\varepsilon} = 1.44, \quad C_{2\varepsilon} = 1.92, \quad C_\mu = 0.09, \quad \sigma_k = 1.0, \quad \sigma_\varepsilon = 1.3$$

The molecular diffusivity of H_2 to air was taken to be D=7.5 10-5 m2/s
During the release the turbulent Schmidt number has been taken equal to 0.7.

The equations have been solved with the SIMPLE method and the convective terms have been discretized using a second order scheme.
The release was modeled with a mass flow inlet condition. After the release this condition was replaced with a wall condition. All values in Table 1 have been modeled appropriately. The further boundary conditions are a constant wall temperature of 20 ºC and smooth walls.
A structured hexahedral mesh was used, except near the injection point. The number of cells was 71561. The grid was refined near the H_2 release and walls. Different views of the mesh used are presented in Figure 9.
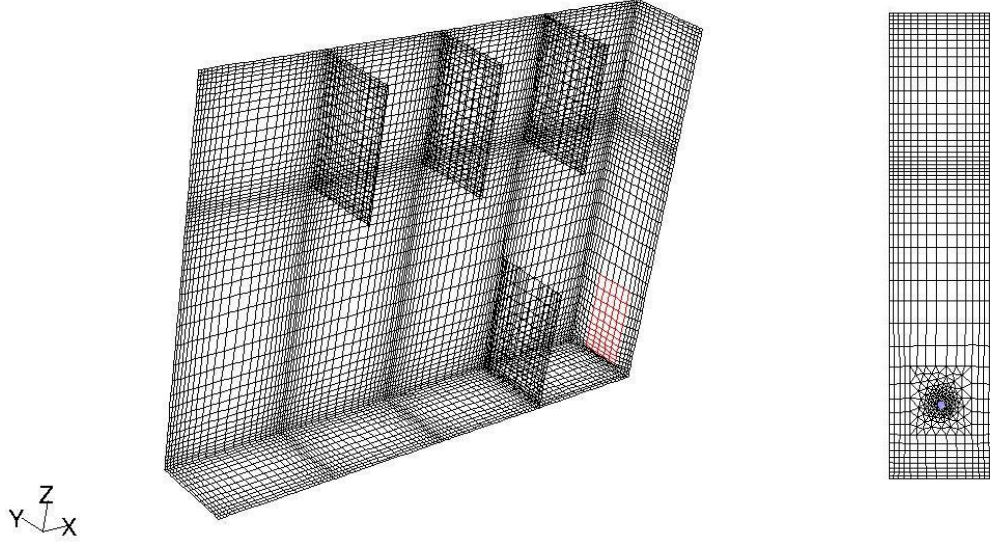
Figure 9 Isometric and front view of the computational grid for Fluent (UPM)

The applied computer equipment was an Linux HP workstation xw6200 with 2 Pentium Xeon Processors and 6GB RAM. The required CPU time was approximately 2 days.

4.5. Numerical modeling of UU

The problem was simulated using general-purpose CFD package FLUENT 6.2.16. The code realises control-volume based finite-difference method. The segregated solver with implicit linearisation of the governing equations was used for simulations. Bounded central difference scheme was used to discretise momentum and hydrogen conservation equations. The value of time step was equal to $\Delta t = 0.01$ s with 40 iterations per time step up to the end of the experimental time. This large time step was needed to perform the simulation in a reasonable time and makes the Large Eddy Simulation (LES) predictions close to those of RANS simulations. The LES model comprised three-dimensional mass, momentum, energy and hydrogen concentration equations:

$$\frac{\partial \overline{\rho}}{\partial t} + \frac{\partial}{\partial x_j}\left(\overline{\rho}\,\widetilde{u}_j\right) = 0 \;,$$

$$\frac{\partial \overline{\rho}\,\widetilde{u}_i}{\partial t} + \frac{\partial}{\partial x_j}\left(\overline{\rho}\,\widetilde{u}_j\widetilde{u}_i\right) = -\frac{\partial \overline{p}}{\partial x_i} + \frac{\partial}{\partial x_j}\left(\mu_{eff}\left(\frac{\partial \widetilde{u}_i}{\partial x_j} + \frac{\partial \widetilde{u}_j}{\partial x_i} - \frac{2}{3}\frac{\partial \widetilde{u}_k}{\partial x_k}\delta_{ij}\right)\right) + \overline{\rho}\,g_i \;,$$

$$\frac{\partial}{\partial t}\left(\overline{\rho}\,\widetilde{E}\right) + \frac{\partial}{\partial x_j}\left(\widetilde{u}_j\left(\overline{\rho}\widetilde{E} + \overline{p}\right)\right) =$$

$$= \frac{\partial}{\partial x_j}\left(\frac{\mu_{eff}c_p}{\mathrm{Pr}_{eff}}\frac{\partial \widetilde{T}}{\partial x_j} - \sum_m \widetilde{h}_m\left(-\frac{\mu_{eff}}{Sc_{eff}}\frac{\partial \widetilde{Y}_m}{\partial x_j}\right) + \widetilde{u}_i\mu_{eff}\left(\frac{\partial \widetilde{u}_i}{\partial x_j} + \frac{\partial \widetilde{u}_j}{\partial x_i} - \frac{2}{3}\frac{\partial \widetilde{u}_k}{\partial x_k}\delta_{ij}\right)\right) \;,$$

$$\frac{\partial}{\partial t}\left(\overline{\rho}\,\widetilde{Y}_{H_2}\right) + \frac{\partial}{\partial x_j}\left(\overline{\rho}\,\widetilde{u}_j\,\widetilde{Y}_{H_2}\right) = \frac{\partial}{\partial x_j}\left(\frac{\mu_{eff}}{Sc_{eff}}\frac{\partial \widetilde{Y}_{H_2}}{\partial x_j}\right) \;.$$

The Smagorinsky-Lilly viscous sub-grid scale model [6] was applied.

Molecular multicomponent diffusivity for hydrogen in air was chosen as $D = 7.5 \cdot 10^{-5}\, \text{m}^2/\text{s}$. Turbulent Schmidt and Prandtl numbers were set to default values Sc_{turb}=0.7 and Pr_{turb}=0.85 accordingly.

The square exit nozzle was modelled with the area equal to the experimental orifice (0.0106 x 0.0106 = $1.13.10^{-4}\, \text{m}^2$). A part of the connecting pipe before experimental rig was modelled to establish velocity profile at the exit nozzle. The pipe length was set to be $L = 0.6$ m.

A structured hexahedral grid was used to mesh the whole calculation domain. The total number of CVs was equal to 261506, with smallest cubic CV side 1.3 mm in the vicinity of the release nozzle. calculation domain included also some free space adjacent to the experimental rig (see Figure 10).

Initial conditions:

- quiescent atmosphere, $u = 0$ m/s,
- initial hydrogen concentration, $Y_{H_2} = 0$,
- initial temperature in the experimental rig T=293 K.
- non-slip, impermeable boundary conditions at walls,
- specified hydrogen concentration $Y_{H_2} = 1.0$ and mass flow rate $\dot{m}$ at inflow:
    - During period $t = 0 - 60$ s, $\dot{m} = 9.89$ kg/s
    - During period $t = 60 - 120$ s, $\dot{m} = 0$ kg/s;
- constant operating pressure $p = 101325$ Pa.,
- constant gauge pressure p=0 Pa at the free space boundaries representing atmosphere.
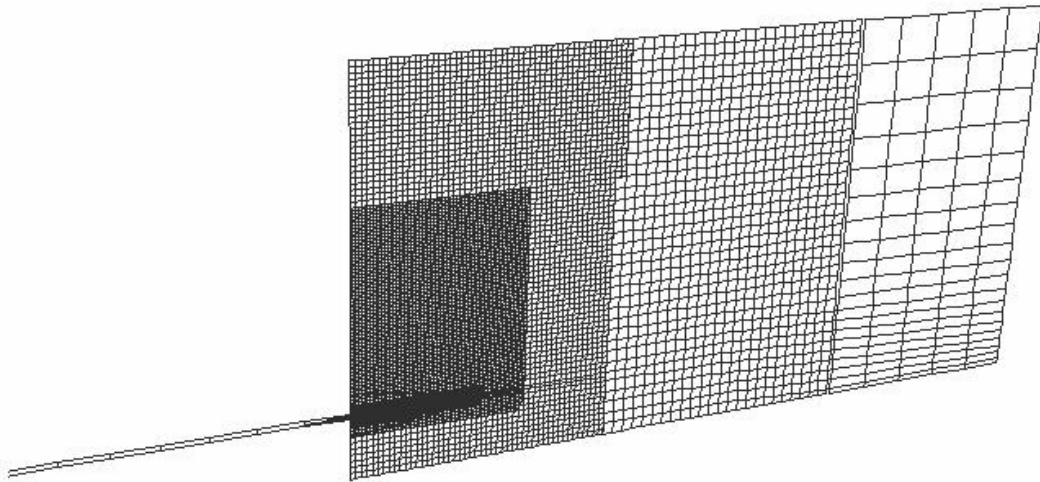

Figure 10 Calculation domain for the Fluent calculation of UU with virtual inlet flow pipe and expansion area

4.6.   *Numerical Modeling of HSE/HSL*

The commercial CFD code CFX release version 10, developed by Ansys, has been used for the dispersion calculations. The Shear Stress Transport (SST) proposed by Menter [7] has been used throughout these simulations. The SST model is a hybrid model that combines the k-ω model of Wilcox with the k-ε model. The boundary condition for ω

goes to infinity in the freestream, which severely limits the application of the original k-ω model. The k-ω model is used in the near-wall region and the k-ε model is used outside the boundary layer.

In the present calculations both production and dissipation due to buoyancy have been taken into account.

The diffusion coefficient, $\mathcal{D}$, is set to constant $7.405 \cdot 10^{-5}$ m^2 s^{-1}, which is applicable at 293.15 K. All walls are solid walls with no-slip conditions. The temperature of the wall is kept at a constant temperature of 20 °C, e.g. 293.15 K. Hence the wall thermal boundary conditions is constant temperature walls at 293.15 K. It has been assumed that the walls are smooth.

It is important that the time step size is not too large. It was necessary to use a small time step, $1.0 \cdot 10^{-4}$ s, during the initial stage of the hydrogen release. The time step could be gradually increased to a maximum of 0.1 s as the simulation progressed.

The four baffles located in the enclosure have finite thickness, given as less than 0.005 m by GexCon, Middha (2006). It was decided to treat the baffles as thin surfaces in the CFD code, which means that the baffles are very thin and thus their thickness does not need to be resolved, which is expedient as it reduces the mesh size. It is possible to specify different boundary conditions on each side of the surface, but here it is appropriate to specify the same constant wall temperature, e.g. 293.15 K, smooth wall and no-slip velocity conditions on both sides of the baffle.

4.7. Numerical Modeling of FZK

First a small sensitivity analysis was conducted with the 3D CFD GASFLOW 2.4 code. For all cases the k-ε-turbulence model was used. The standard settings of the GASFLOW implementation differ slightly from the actual standard settings.

Case	Inflow H_2-T (°C)	Turb. Schmidt	Heat Trans-fer	Mesh	Comments and Effects
1 (reference)	20	0.85	No	Coarse 55x42x10 = 23100	1. Uses GASFLOW default values 2. Steady State #9 & #10 between 33% & 34%, respectively. 3. #10 slightly higher than #9 in contrast with data.
2	20	1.50	No	Coarse 55x42x10 = 23100	1. Increases #9 to 35%, and #10 to 36% 2. #10 slightly higher than #9 in contrast with data.
3	0	0.85	No	Coarse 55x42x10 = 23100	1. Increases #9 to 34%, and #10 to 35% 2. #10 slightly higher than #9 in contrast with data.
4	0	1.00	No	Coarse 55x42x10 = 23100	1. Increases #9 to 35%, and #10 to 36% 2. #10 slightly higher than #9 in contrast with data.
5	0	0.85	Yes	Coarse 55x42x10 = 23100	1. Increases #9 to 34%, and #10 to 36% 2. #10 slightly higher than #9 in contrast with data.

| 6 | 20 | 0.85 | No | Fine 80x63x15 = 75600 | 1. Same as reference Case 1 with finer spatial resolution
2. Steady State #9 & #10 between 35% & 34%, respectively.
3. #9 slightly higher than #10 in agreement with data. |

Table 2: Release conditions

Table 2 Summarises the results of the sensitivity analysis. All further results refer to case 1 as the refernce case. Changing the turbulent Schmidt number, the inflow temperature, the energy transport or the mesh yields only small but positive effects when comparing to the experimenal data.

4.8.   *Summary of the simulation characteristcs*

Some key elements of the above described simulations are summarised in Table 3 below.

CODE (Partner)	Mesh cell number	Maximum/ minimum cell dimensions	Turbulence Model	CPU time / special
ADREA- (NCSRD)	141.466	12 mm	standard k-ε	
FLACS (GexCon)	38.318	11 mm	-	64 h
KFX (DNV)	15.444	11-30 mm	standard k-ε	
FLACS (DNV)	15.444	15 mm	-	
FLUENT (UPM)	71.561		standard k-ε	48 h
FLUENT (UU)	261.506	1,3 mm	LES	
CFX (HSE/HSL)		0,5-2 mm	SST	
GASFLOW (FZK)	23.100	15 mm	k-ε	

Table 3: Summary of simulation characteristics

5.   COMPARISON OF THE RESULTS

The results of the different numerical simulations are compared against each other and against the experimental data. The results are summarized in 4 Figures 11.a-d
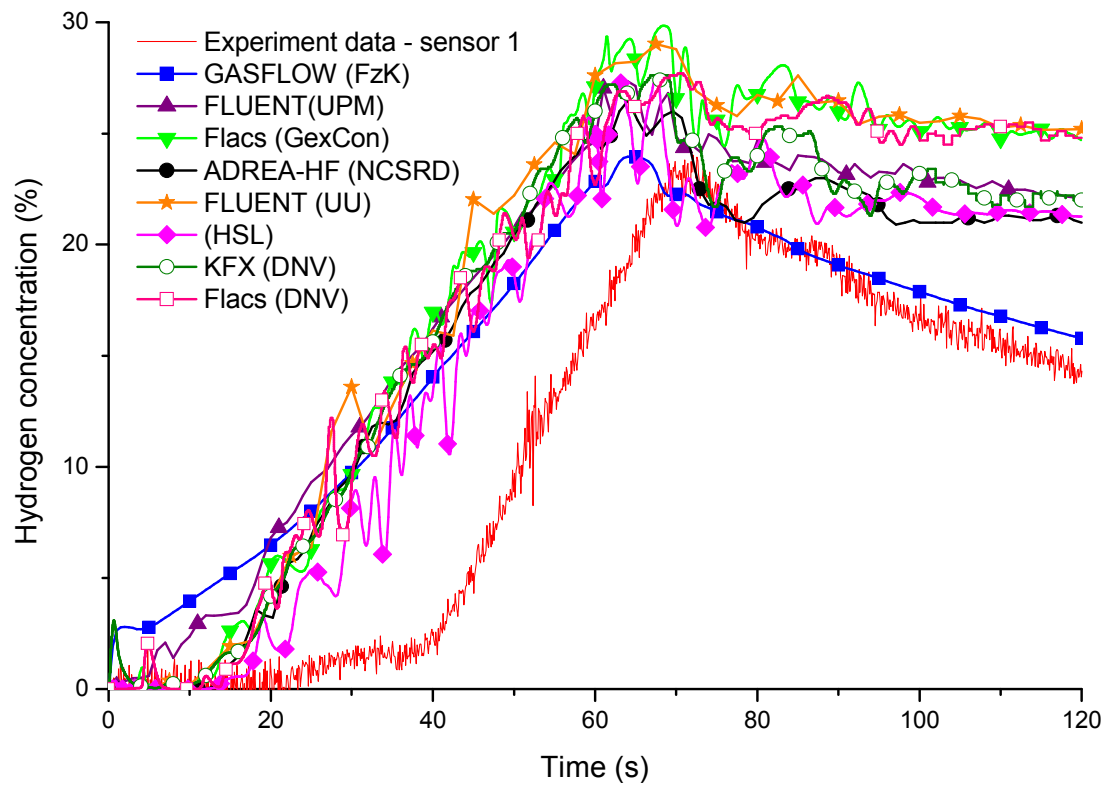
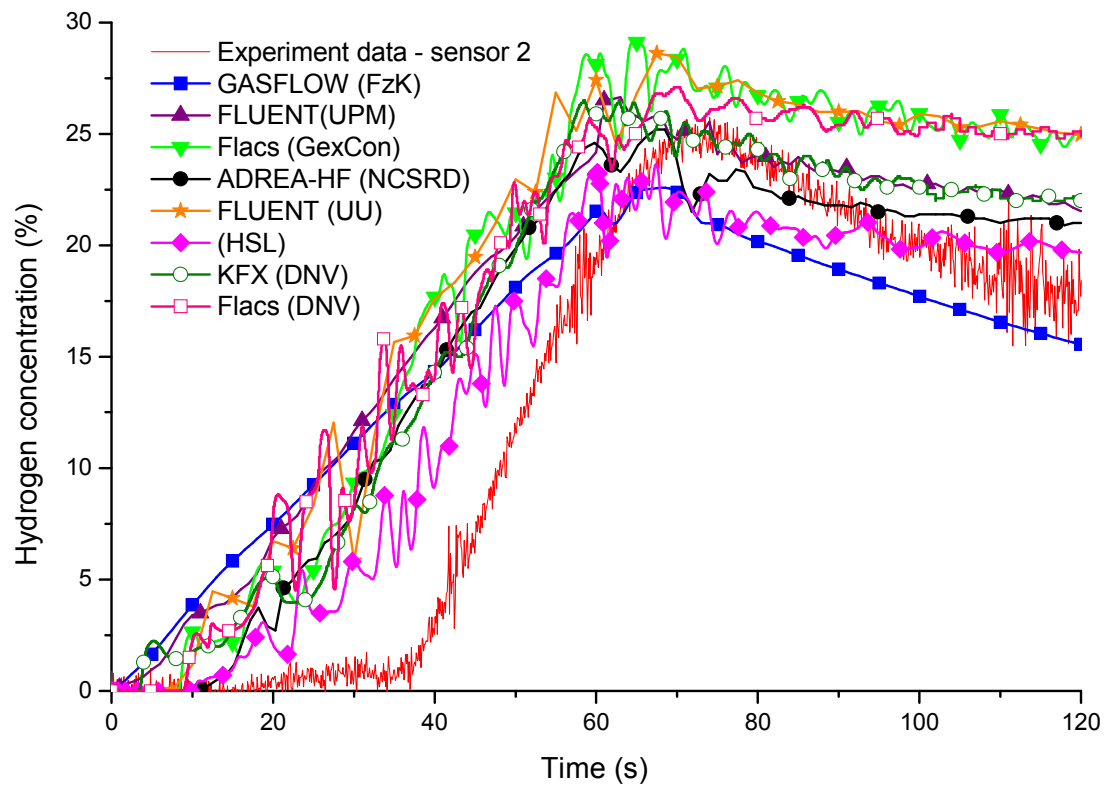**Figure 11.a Calculated and measured H$_2$ concentrations versus time at sensor 1**

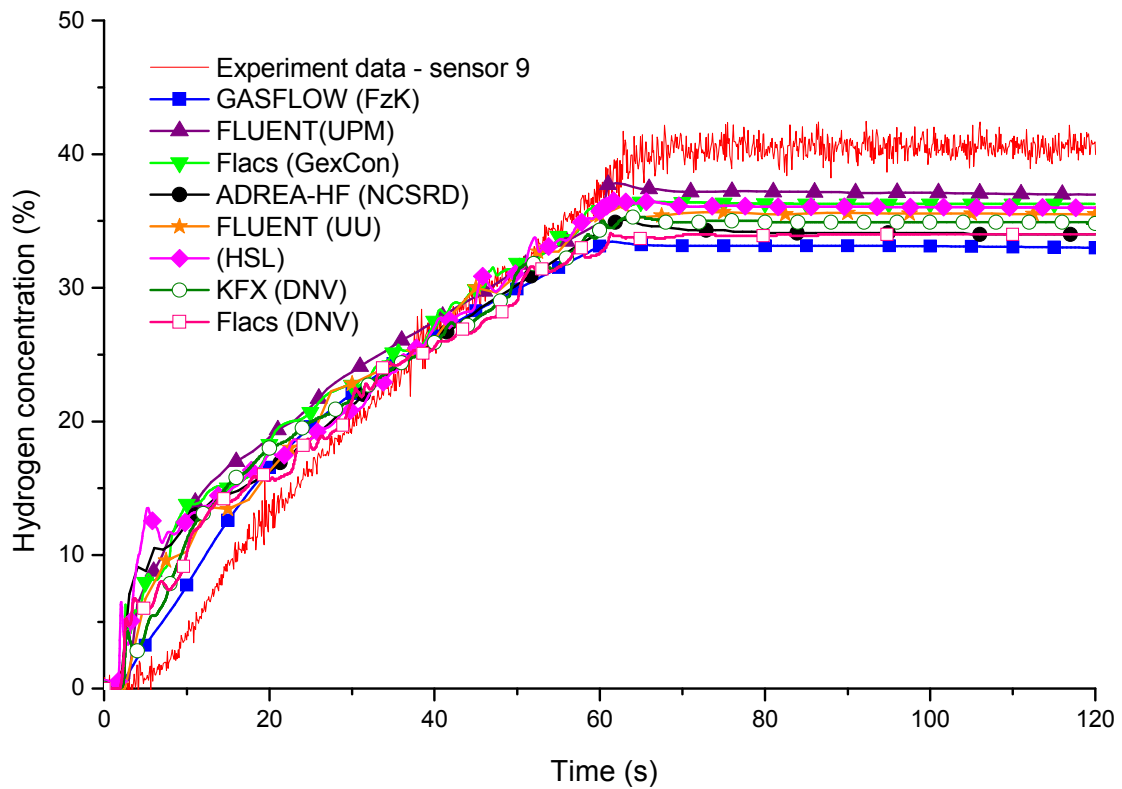**Figure 11.b Calculated and measured H$_2$ concentrations versus time at sensor 2**

Figure 11.c Calculated and measured H$_2$ concentrations versus time at sensor 9
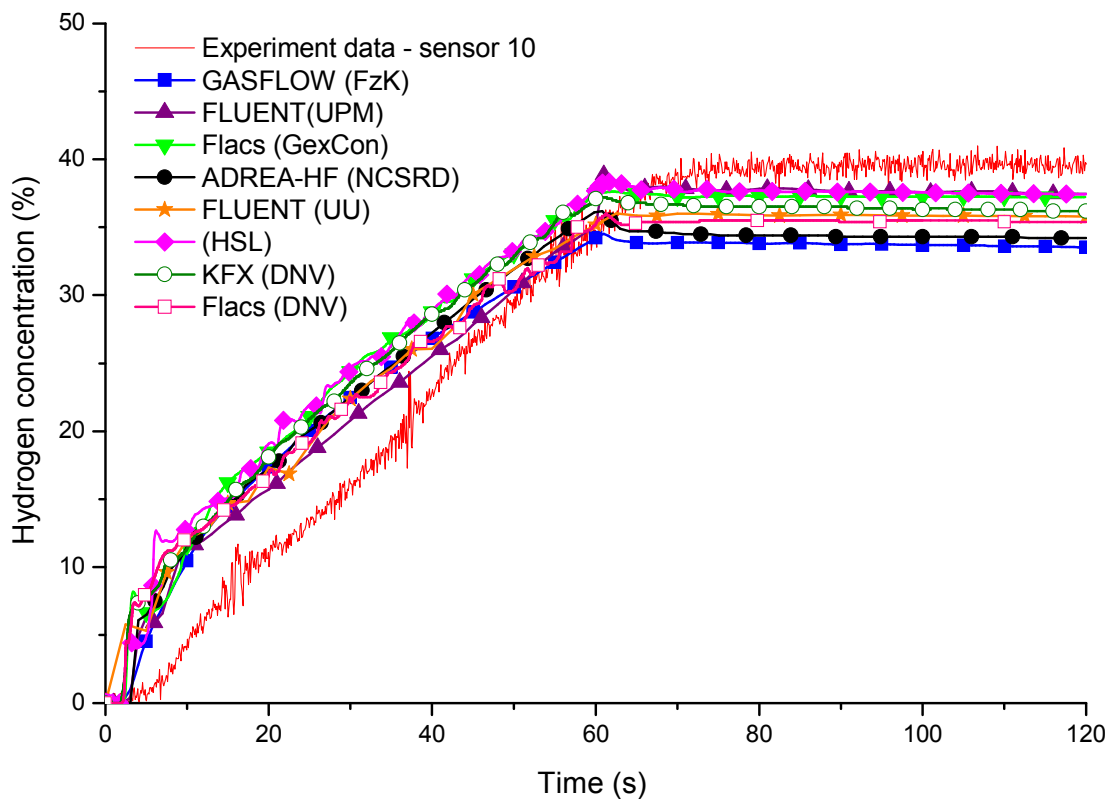

Figure 11.d Calculated and measured H$_2$ concentrations versus time at sensor 10

For the sensors 1 and 2 with their position in the jet direction a delay of nearly 40 seconds in the rise of concentrations is observed. The time of arrival of the maximum concentrations in the most sensitive positions 9 and 10 coincide for all calculations surprisingly well. The time to reach a concentration of 15% at the same locations is predicted in between 16 to 19 seconds for sensor 9, 17 to 20 seconds for sensor 10 after release start. For sensor 9 the experimental and computational results are closer during the release phase than after the release with the steady state concentrations. For sensor 10 this trend is opposite.

6.   CONCLUSIONS

In advance some dispersion experiments were carried out by two HySafe partners in a small-scale vessel with 4 baffles in order to determine the concentration distribution as a function of time. Only natural ventilation in the form of an opening is present. The experiment is simple, well documented, and well instrumented, except for the failure of a few sensors. Therefore it was selected as a suitable case to validate CFD codes.

The CFD simulation results compare reasonably well with experimental data. Some discrepancies are seen, especially for sensors 1 and 2 close to the horizontal jet release. Some of these discrepancies may be attributed to experimental uncertainties, especially the response time and transient precision of the various sensors are unknown and seem to influence the experimental data.

Also, the scatter in the jet release domain within the simulation results is stronger, what indicates the importance of a careful modeling of the source, in particular of the horizontal jet. However, in general the scatter in the simulation results is reasonably small and largely understood what additionally supports to question some aspects of the experimental measurements.
The understanding of the remaining scatter is based on the experience obtained by the previous benchmark excersises and on the outcome of the sensitivity analyses:
1. a hydrogen inflow temperature variation (between 0°C and 20 °C) results in a positive, but small effect,
2. increasing the turbulent Schmidt Number from 0,7 to 1,5 results in a positive, but small effect,
3. considering structural heat transfer results in a positive, but small effect.
5. increasing mesh resolution from charcteristically 15mm by 50% in all dimensions results in a positive, but small effect with the k-ε turbulence models.

The concentrations in the locations 9 and 10 reach a steady state which is satisfactorily models by all codes. As the baffle plate between these two compartments lies right in the rising jet release the concentrations in these locations are a sensitive indicator for a good buoyant jet modeling. The standard k-ε turbulence model results and these provided with the only LES simulation coincide very well. This supports the positive message that for these kind of scenarios the usage of the standard industry turbulence model is possible.

These results additionally supported to start more detailed analyses of horizontal strong buoyant jets.

7.   ACKNOWLEDGEMENT

8.   REFERENCES

[1] NoE HySafe website www.hysafe.net

[2] Industrial Scientific Oldham website www.groupoldham.com/site_en/frame.php

[3] G. Bartzis, "ADREA-HF: A three dimensional finite volume code for vapour cloud dispersion in complex terrain", EUR report 13580 EN, 1991

[4] Launder B.E. and Spalding D.B., "The numerical computation of turbulent flow", Computer Methods in Applied Mechanics and Engineering, 3, Issue 2, pp. 269-289

[5] Patankar, S. V., "Numerical heat transfer and fluid flow", Hemisphere Publishing Corporation, 1980

[6] Smagorinsky J.. General Circulation Experiments with the Primitive Equations. I. The Basic Experiment. *Month. Wea. Rev.*, 91:99-164, 1963.

[7] Menter, F. R., "2-Equation Eddy-Viscosity Turbulence Models For Engineering Applications", AIAA Journal, Vol. 32, No. 5, pp. 1598-1605, 1994